GRID-SEARCH TECHNIQUES FOR SEISMIC EVENT LOCATION

William Rodi and M. Nafi Toksöz
Earth Resources Laboratory
Massachusetts Institute of Technology

Sponsored by The Defense Threat Reduction Agency
Arms Control Technology Division
Nuclear Treaties Branch
Contract pending

U.C. Lawrence Livermore National Laboratory
Subcontract No. B506161

ABSTRACT

We are developing a new algorithm for seismic event location to address particular problems of importance in monitoring the Comprehensive Nuclear-Test-Ban Treaty, including the assessment of location accuracy and increasing the number of seismic phases used for location. Our approach is formulated within a maximum-likelihood estimation framework and implemented numerically with grid-search and Monte Carlo techniques. It obtains globally optimal hypocentral estimates and non-ellipsoidal confidence regions that do not depend on the usual assumption of local linearity of the forward problem. The approach accommodates such complexities as 3-D traveltime tables, non-Gaussian data errors, and general types of parameter constraints. Specific problems we are addressing are (1) extension of our uncertainty analysis to account more realistically for the effects of modeling errors (errors in traveltime tables), which traditionally have not been distinguished from random picking errors in the determination of location confidence regions; (2) incorporation of azimuth and slowness data, in addition to arrival times, into the maximum-likelihood framework; and (3) integration of phase association into the event location algorithm in order to perform these tasks simultaneously with a grid-search approach. We present examples of our event location algorithm applied to data from the International Monitoring System, illustrating the effects of nonlinearity on hypocentral confidence regions determined from sparse data sets.

Key words: seismic, event location, confidence region, grid search, CTBT

OBJECTIVE

Over the past decade, grid search has gained popularity as an inversion algorithm for seismic event location, owing to its simplicity of implementation and ability to find globally optimal hypocentral estimates. Unlike the traditional iterative methods, grid search easily accommodates problem complexities such as general error models (non-Gaussian), nonlinear parameter constraints, and multiple data types (azimuth and slowness in addition to arrival times). One of the early applications of the method was the work of Sambridge and Kennett (1986), who applied a directed grid-search technique to teleseismic location. Recently, Dreger *et al.* (1998) applied grid search to problems of event location with sparse regional networks, an important situation in CTBT monitoring. Previous applications of grid search in event location were formulated to minimize a "data misfit" function with respect to hypocentral parameters. Contours of this function were recognized to approximate the boundaries of confidence regions, to which confidence levels could be assigned within certain linear approximations and under the assumption of Gaussian errors (Wilcock and Toomey, 1991).

We are developing a more general algorithm for event location that uses grid search to maximize a general likelihood function. Maximum likelihood estimation theory provides a formal framework for non-Gaussian error assumptions and for combining diverse types of data and prior information on parameters. In addition, our algorithm replaces approximate, analytical formulas for confidence levels with Monte Carlo simulation, which is not restricted by the Gaussian assumption and which accounts fully for nonlinearity of the forward problem and parameter constraints. Other enhancements in progress or planned for the near future include the incorporation of azimuth and slowness data, a more complete treatment of the errors in traveltime tables sued for forward modeling, and integration of seismic phase association tasks into our grid-search algorithm in an attempt to constrain event locations with more seismic phases. Our objective is improved location accuracy and more realistic analyses of location error for small, sparsely recorded events.

RESEARCH ACCOMPLISHED

Maximum Likelihood Formulation

The hypocentral parameters of a seismic event are a three-dimensional position vector $\mathbf{x}$ and an origin time t. Let $\mathbf{d} = (d_1, d_2 \ldots, d_n)$ be an n-dimensional vector of arrival times picked from various seismic phases at a seismic network. The event location problem may be expressed as

$$d_i = t + T_i(\mathbf{x}) + e_i, \quad i = 1, \ldots, n \tag{1}$$

where T_i is a traveltime function (traveltime table) for the ith datum and e_i is an error with respect to this function. The index i counts over both stations and phase types (P, S, etc.), including only those combinations that have been actually observed (i.e., completeness of data coverage is not assumed).

We assume the errors are statistically independent and, following Billings *et al.* (1994), that each is distributed with a "generalized Gaussian" probability density function (p.d.f.) given by

$$\mathrm{pdf}(e_i) = \frac{1}{K\sigma_i} \exp\left\{ -\frac{1}{p} \left| \frac{e_i}{\sigma_i} \right|^p \right\} \tag{2}$$

where $K = 2p^{1/p}\Gamma(1 + 1/p)$ and Γ is the gamma function. When $p = 2$, then e_i is normally distributed with zero mean and variance $(\sigma_i)^2$. When $p = 1$, it is exponentially distributed. We assume that the scale parameters σ_i are known in a relative sense and write

$$\sigma_i = \sigma\nu_i \tag{3}$$

where the ν_i are known but the universal scale parameter, σ, is not.

The joint p.d.f. of the n data is the product of the error p.d.f.'s. Considered as a function of the unknown parameters ($\mathbf{x}$, t and σ) this joint p.d.f. is a *likelihood* function, which we denote as $L(\mathbf{x}, t, \sigma; \mathbf{d})$. It is convenient to deal with the negative logarithm of likelihood, which we denote as Λ. This is given by

$$\begin{aligned} \Lambda(\mathbf{x}, t, \sigma; \mathbf{d}) &\equiv -\log L(\mathbf{x}, t, \sigma; \mathbf{d}) \\ &= \sum_{i=1}^{n} \log \nu_i + n \log K + n \log \sigma + \frac{1}{p\sigma^p} \Psi(\mathbf{x}, t; \mathbf{d}) \end{aligned} \tag{4}$$

Here, Ψ is a 'data misfit' function defined as

$$\Psi(\mathbf{x}, t; \mathbf{d}) = \sum_{i=1}^{n} |d_i - t - T_i(\mathbf{x})|^p / (\nu_i)^p. \tag{5}$$

The maximum likelihood estimates of the unknowns are the values that maximize L or, equivalently, *minimize* Λ. We denote these estimates as $\mathbf{x}_{ml}$, t_{ml}, and σ_{ml}. The maximization may be subjected to prior constraints on the parameters. In our current algorithm, we assume hard upper and lower bounds on focal depth (z) and the p.d.f. scale factor:

$$0 \leq z \leq z^{max} \tag{6}$$

$$\sigma^{min} \leq \sigma \leq \sigma^{max}. \tag{7}$$

We allow latitude and longitude to be anywhere on the globe, or restricted to within a given distance of a given geographic location. We place no constraint on origin time.

Given its structure, Λ is amenable to a hierarchical minimization with respect to the unknown parameters, leading to minimization subproblems of lower dimension than the original problem. We define a "reduced" objective function which, for each fixed hypocenter, is minimum with respect to t and σ (subject to prior constraints on σ):

$$\widetilde{\Lambda}(\mathbf{x};\mathbf{d}) = \min_{t,\sigma} \Lambda(\mathbf{x}, t, \sigma; \mathbf{d}). \tag{8}$$

The location problem reduces to minimization of $\widetilde{\Lambda}$.

Grid Search

Our current grid search algorithm obtains the maximum likelihood estimates of the hypocentral parameters ($\mathbf{x}_{ml}$ and t_{ml}) and the p.d.f. scale parameter (σ_{ml}), as defined in the previous section. The algorithm computes the reduced objective function, $\widetilde{\Lambda}$ in equation (8), at each point in a 3-D grid of hypocenters. Following previous workers, the hypocenter grid is constructed dynamically through a process of successive refinement. Our procedure for grid refinement resembles that of the 'neighborhood' search algorithm developed by Sambridge (1999). The first grid covers the entire globe and from 0 to 700 km in depth at coarse spacing: 100 km in depth, 9 degrees in latitude, and 9 degrees in longitude near the equator and increasing at higher latitudes. On each pass of grid refinement, nodes are added as neighbors of a subset of grid points comprising the "best" (smallest $\widetilde{\Lambda}$) points tested thus far. Neighbors are placed at one-third the grid-spacing of the previous pass. The size of the grid subset chosen for refinement is reduced on each pass. The search ends when the grid spacing is less than 0.3 km.

Non-Ellipsoidal Confidence Regions

A confidence region on the hypocenter of an event is defined classically in terms of a statistic, τ, that is a function of the data vector, $\mathbf{d}$, and the hypocenter, $\mathbf{x}$. A confidence region at confidence level $1-\alpha$ comprises those values of $\mathbf{x}$ satisfying the inequality

$$\mathrm{cdf}(\tau(\mathbf{d},\mathbf{x})) \leq 1-\alpha. \tag{9}$$

Here, cdf denotes the cumulative distribution function of a random variable.

Flinn (1965) defined hypocentral confidence regions for the case of Gaussian errors ($p=2$) and no prior bounds on σ ($\sigma^{min}=0$, $\sigma^{max}=\infty$). Evernden (1969) treated the case with σ completely known ($\sigma = \sigma^{min} = \sigma^{max} = \sigma_{ml}$), while Jordan and Sverdrup (1981) generalized these two results to account for partial prior knowledge of σ. The statistic used by each of these workers can be expressed in our notation as

$$\tau(\mathbf{d},\mathbf{x}) = \frac{\widetilde{\Psi}(\mathbf{x};d) - \widetilde{\Psi}(\mathbf{x}_{ml};d)}{\sigma^2_{ml}} \tag{10}$$

where $\widetilde{\Psi}$ is the "reduced" data misfit function (Ψ minimized with respect to t for each fixed $\mathbf{x}$). Under the approximation that the traveltime functions, $T_i(\mathbf{x})$, are locally linear near $\mathbf{x} = \mathbf{x}_{ml}$, the probability distribution of τ does not depend on any of the unknown parameters ($\mathbf{x}$, t or σ), and a confidence region takes the form

$$\widetilde{\Psi}(\mathbf{x};\mathbf{d}) - \widetilde{\Psi}(\mathbf{x}_{ml};\mathbf{d}) \leq \sigma_{ml}^2 C_\alpha \tag{11}$$

where C_α is a constant. Under the linearity assumption, this equation defines a hyper-ellipsoid in hypocenter space. Flinn (1965), Evernden (1969), and Jordan and Sverdrup (1981) derive different values of C_α based on differing assumptions about σ.

To test the linear approximation, Wilcock and Toomey (1991) computed non-ellipsoidal confidence regions directly from equation (11). This equation implies that each surface of constant data misfit, $\widetilde{\Psi}(\mathbf{x};\mathbf{d})$, is the boundary of a confidence region for some level of confidence, $1-\alpha$. They directly sampled $\widetilde{\Psi}(\mathbf{x};\mathbf{d})$ on a grid of hypocenters to map the non-ellipsoidal confidence region for a fixed confidence level, thus taking the major effect of nonlinearity into account. However, the approach of Wilcock and Toomey (1991) ignores another effect of nonlinearity: the probability distribution of τ may depend on the true values of the unknown parameters. This effect can be caused by the use of nonlinear constraints on the parameters, as in eqs. (6) and (7), as well as by nonlinearity of the traveltime functions. Moreover, they did not consider the case of non-Gaussian errors.

We have generalized the approach of Wilcock and Toomey as follows. We define a test statistic as the logarithm of a likelihood ratio:

$$\begin{aligned}\tau(\mathbf{d},\mathbf{x}) &= \log\left[\frac{\max_{\mathbf{x},t,\sigma} L(\mathbf{x},t,\sigma;\mathbf{d})}{\max_{t,\sigma} L(\mathbf{x},t,\sigma,\mathbf{d})}\right] \\ &= \widetilde{\Lambda}(\mathbf{x};\mathbf{d}) - \widetilde{\Lambda}(\mathbf{x}_{ml};\mathbf{d}).\end{aligned} \tag{12}$$

That is, τ differences our reduced objective function between $\mathbf{x}$ and the maximum likelihood solution, $\mathbf{x}_{ml}$. This statistic is equivalent to the ones used by Flinn and Evernden under their respective assumptions about σ, but accommodates arbitrary constraints on the parameters and non-Gaussian error distributions. Letting $\mathbf{x} = (x, y, z)$, the statistic for a 2-D confidence region on the event epicenter, (x, y), is given by

$$\tau(\mathbf{d},x,y) = \min_z \widetilde{\Lambda}(\mathbf{x};\mathbf{d}) - \widetilde{\Lambda}(\mathbf{x}_{ml};\mathbf{d}) \tag{13}$$

and for a confidence interval on focal depth is

$$\tau(\mathbf{d},z) = \min_{x,y} \widetilde{\Lambda}(\mathbf{x};\mathbf{d}) - \widetilde{\Lambda}(\mathbf{x}_{ml};\mathbf{d}). \tag{14}$$

Confidence regions using these log-likelihood statistics could still be defined via the inequality of equation (9), except this inequality presumes that the distribution (c.d.f.) of τ does not depend on the true values of the parameters. We assume the main dependence is on focal depth and σ, and write the c.d.f. of τ as $\mathrm{cdf}(\tau; z, \sigma)$. We generalize the inequality of equation (9) to use the c.d.f. of τ that is minimum with respect to the true parameters. Thus, the hypocentral confidence region is given by

$$\min_\sigma \mathrm{cdf}(\tau(\mathbf{d},\mathbf{x}); z, \sigma) \leq 1-\alpha. \tag{15}$$

The epicentral one is

$$\min_{\sigma,z} \mathrm{cdf}(\tau(\mathbf{d},x,y); z, \sigma) \leq 1-\alpha, \tag{16}$$

and the focal depth confidence interval is

$$\min_{\sigma} \mathrm{cdf}(\tau(\mathbf{d}, z); z, \sigma) \leq 1 - \alpha. \tag{17}$$

With these definitions, a confidence region will include the true value of the parameter *at least* $100(1-\alpha)$ percent of the time.

Confidence Regions Via Monte Carlo Sampling

We outline the technique for hypocentral confidence regions. The basic idea is to estimate the c.d.f. of the test statistic τ by simulation, i.e. computing τ for many randomly generated samples of the error vector. We generate each error, e_i^{mc}, using a pseudo-random number generator in accordance with the assumed error distribution (eqs. (2)–(3)) for some given "true" σ. Then, for given true hypocentral parameters, $\mathbf{x}$ and t, synthetic data are calculated as

$$d_i^{mc} = t + T_i(\mathbf{x}) + e_i^{mc}. \tag{18}$$

We apply our grid search algorithm to these data to obtain the m.l. hypocenter, $\mathbf{x}_{ml}^{mc}$. Plugging this into the formula for τ,

$$\tau(\mathbf{d}^{mc}, \mathbf{x}) = \widetilde{\Lambda}(\mathbf{x}; \mathbf{d}^{mc}) - \widetilde{\Lambda}(\mathbf{x}_{ml}^{mc}; \mathbf{d}^{mc}). \tag{19}$$

we obtain one sample from $\mathrm{cdf}(\tau; z, \sigma)$. We compare this sample to the observed value of the statistic, $\tau(\mathbf{d}, \mathbf{x})$, obtained from the real data. We count a rejection of $\mathbf{x}$ if

$$\tau(d^{mc}, \mathbf{x}) < \tau(\mathbf{d}, \mathbf{x}). \tag{20}$$

The fraction of rejections after many Monte Carlo trials yields an estimate of $\mathrm{cdf}(\tau(\mathbf{d}, \mathbf{x}); z, \sigma)$. Performing this simulation for multiple values of σ and then minimizing amongst them gives the *lowest* confidence level such that the confidence region includes $\mathbf{x}$. The process for depth confidence intervals and epicenter confidence regions proceeds in the same manner, except that in the latter case the simulation is performed for multiple values of true depth as well as σ, and the confidence level is minimized over both.

Examples With IMS Data

We illustrate our grid-search/Monte Carlo event location algorithm on two events from the Prototype International Data Center (PIDC) Reviewed Event Bulletin (REB). The first is event number 20354875, which occurred 1 March 1999 near Crete and was assigned a magnitude of $m_b = 3.9$. The International Monitoring System (IMS) location is based on five arrival times: Pn at stations BRAR ($\Delta = 7.2°$) and KVAR ($\Delta = 15.7°$), and P at BGCA ($\Delta = 30.6°$), ARCES ($\Delta = 34.5°$) and DBIC ($\Delta = 40.0°$). We applied our grid-search location algorithm to this event using the IASPEI91 traveltime tables and with no elevation or path corrections applied to the data. Arrival time errors were assumed to be Gaussian ($p = 2$) with standard deviation (σ) bounded between 0.5 and 1.5 seconds.

Figure 1 displays confidence level as a function of event location, computed via Monte Carlo simulation. The simulations were performed with three hypothesized "true" values of σ and 6 values of focal depth. The number of error realizations for each σ and z was 300. The top left panel displays confidence level as a function of event depth. The two points where the curve intersects a given confidence level are the end-points of the focal depth confidence interval at that level. The

90% confidence interval on the focal depth of this event is 34 to 92 km, while the 95% interval is 0 to 101 km. The IMS solution fixed the depth to zero.

The upper right panels show cross-sections of confidence levels on the 3-D hypocenter. In each plot, a contour of constant confidence level outlines the boundary of the hypocentral confidence region at that level. The REB solution for the hypocenter is plotted as a circle. We see that the hypocentral confidence regions display significant departure from ellipsoidal behavior. Significantly, the effect is to stretch the confidence regions towards the earth's surface, making it more difficult to reject a shallow focus.

The bottom panels are confidence level as a function of event epicenter, whose contours define epicentral confidence regions at various levels. In the bottom left panel, depth is unconstrained ($z \geq 0$) as in the usual definition of an epicentral confidence region. We see that these confidence regions are close to ellipsoidal and indicate roughly the same epicentral uncertainty as the REB, which reports semi-axes of 57 and 22 km for the 90% confidence ellipse. In the lower right panel, depth is constrained to be shallow ($0 \leq z \leq 10$ km). The title above the plot indicates that a shallow focus can be rejected with a confidence of 83%. However, the plot shows that this low confidence pertains only to a small epicentral region, much smaller than the epicentral confidence region for unconstrained depth (lower left). Thus, the epicenter pertinent to a shallow focus event is much better determined.

A second example of Monte Carlo confidence regions is shown in Figure 2. These are for an $m_b = 3.7$ event in the Afghanistan-Tajikistan border region (17 March 1999, event no. 20380677 from PIDC). The data set comprised five P wave arrival times, all teleseismic except station NIL ($\Delta = 5.1°$). The REB solution reports semi-axes of 92 and 33 km for the 90% confidence region on epicenter. This is consistent with but somewhat larger than the epicentral uncertainty implied in the lower left panel. The REB confidence interval on depth is 35 to 130 km, compared to our smaller 52 to 116 km confidence interval (upper left panel of Figure 2). Our smaller location uncertainties may be due to a more optimistic assumption about data errors (0.5 to 1.5 s) than used in the IMS location algorithm. Looking at the lower right panel, we see that a shallow focus is rejected with 98% confidence, and essentially with 100% confidence outside an elliptical region northeast of the unconstrained solution.

CONCLUSIONS AND RECOMMENDATIONS

We have developed a general theoretical and computational framework for finding event location estimates and confidence regions, relaxing some of the assumptions currently used in the routine processing of IMS data. In particular, we do not assume local linearity of forward problem (traveltime vs. hypocenter) in the computation of confidence regions, and we accommodate fairly general error models and parameter constraints. Our preliminary tests show consistency with IMS results reported in the Reviewed Event Bulletin, but also some noticeable departures from the ellipsoidal confidence regions computed by IMS when small data sets are used.

Currently we are incorporating azimuth and slowness data into our formulation and algorithms. Such data are routinely used in IMS processing and can provide important constraints on sparsely recorded, small events. We are beginning to address some additional, difficult problems of importance in CTBT monitoring. One is the effect of errors in station corrections and traveltime tables ("modeling" errors) on location accuracy. In current location algorithms, modeling errors are accounted by inflating the variances assigned to the data, thus assuming they are random and independent between stations and phases. We will investigate more realistic treatments of these errors that are consistent with empirical analyses of traveltime residuals and calibration studies. The second problem to address is unassociated and mis-associated seismic phases. Our goal is to

integrate key elements of seismic phase association into the process of event location in an attempt to constrain locations with more data and, accordingly, leave fewer unassociated phases in the arrival bulletins. Our maximum likelihood formulations and grid-search approach to event location provides a flexible framework for addressing these problems.

References

[1] Billings, S.D., M.S. Sambridge and B.L.N. Kennett, 1994, Errors in hypocenter location: picking, model and magnitude dependence, *Bull. Seism. Soc. Am., 84,* 1978–1990.

[2] Dreger, D., R. Uhrhammer, M. Pasyanos, J. Franck and V. Romanowicz, 1998, Regional and far-regional earthquake locations and source parameters using sparse broadband networks: a test on the Ridgecrest sequence, *Bull. Seism. Soc. Am., 88,* 1353–1362.

[3] Evernden, J.F., 1969, Identification of earthquakes and explosions by use of teleseismic data, *J. Geophys. Res., 74,* 3828–3856.

[4] Flinn, E.A., 1965, Confidence regions and error determinations for seismic event location, *Rev. Geophys., 3,* 157–185.

[5] Jordan, T.H. and K.A. Sverdrup, 1981, Teleseismic location techniques and their application to earthquake clusters in the south-central Pacific, *Bull. Seism. Soc. Am., 71,* 1105–1130.

[6] Sambridge, M., 1999, Geophysical inversion with a neighbourhood algorithm—1. Searching a parameter space, *Geophys. J. Int., 138,* 479–494.

[7] Sambridge, M.S. and B.L.N. Kennett, 1986, A novel method of hypocentre location, *Geophys. J.R. astr. Soc., 87,* 679–697.

[8] Wilcock, W.S.D. and D.R. Toomey, 1991, Estimating hypocentral uncertainties for marine microearthquake surveys: a comparison of the generalized inverse and grid search methods, *Marine Geophysical Researches, 13,* 161–171.

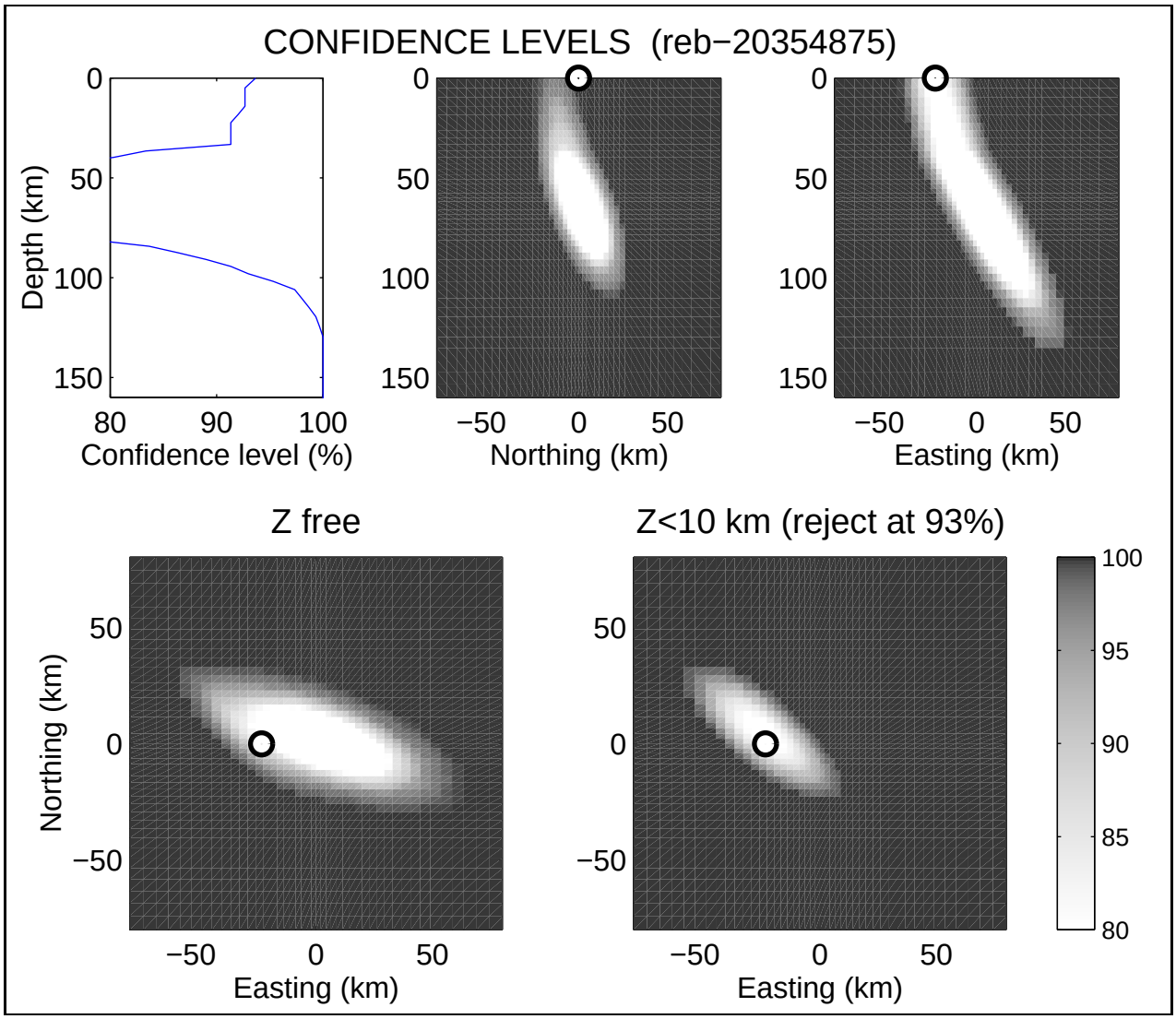

Figure 1: Confidence level vs. location for an $m_b = 3.9$ event near Crete (1 March 1999, event no. 20354875 from PIDC). *Top left:* Confidence level vs. focal depth. *Top center and right:* cross-sections of confidence level vs. hypocenter. *Bottom left:* Confidence level vs. epicenter. *Bottom right:* Confidence level vs. epicenter with focal depth constrained between 0 and 10 km. In the top images, each contour of constant confidence level intersects the boundary of the 3-D hypocentral confidence region at that level. Contours in the bottom images are the boundaries of epicentral confidence regions. Note that confidence levels below 80% are all displayed with white. The circles mark the event hypocenter reported in the Reviewed Event Bulletin.

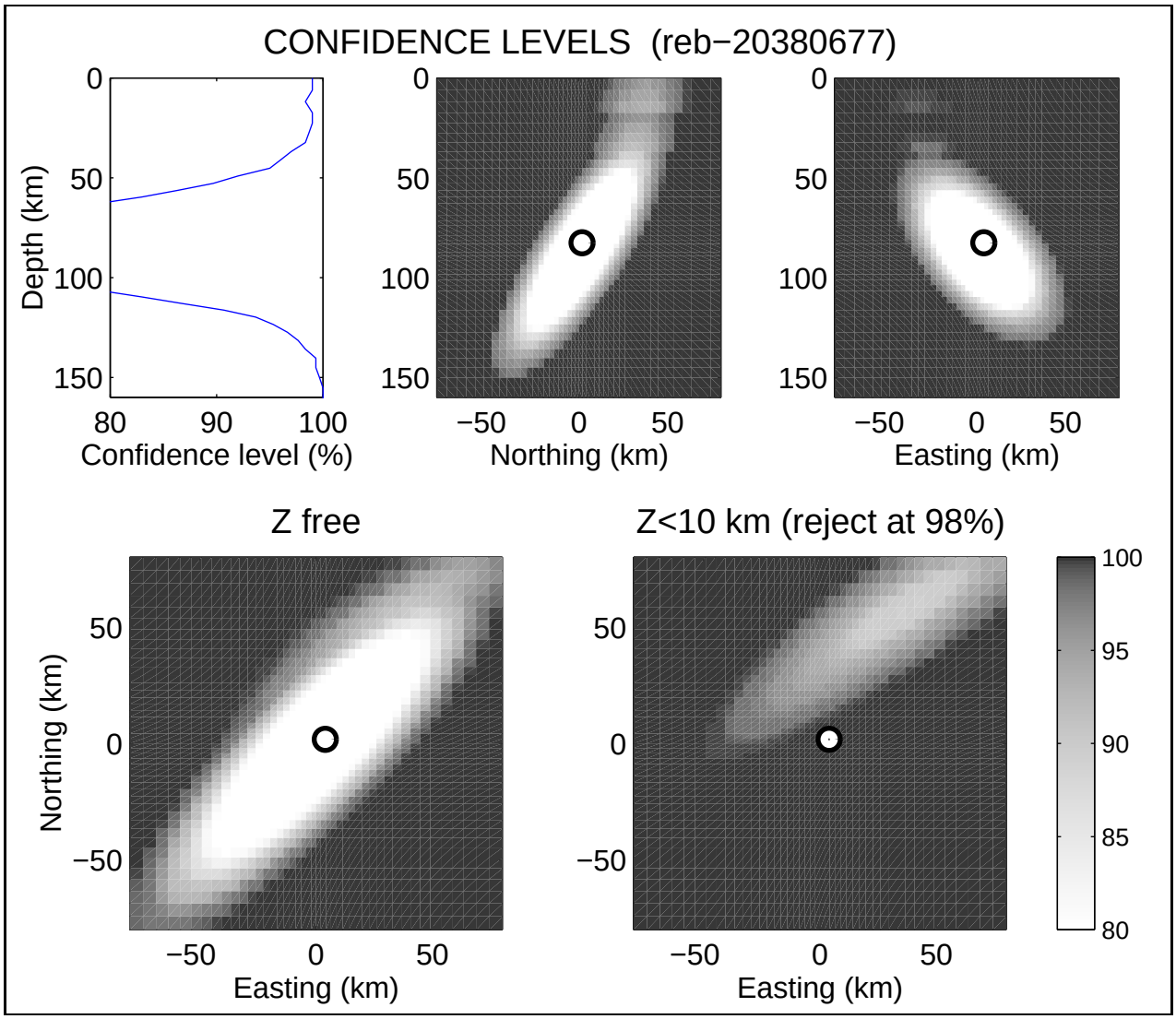

Figure 2: Confidence level vs. location for an $m_b = 3.7$ event in the Afghanistan-Tajikistan border region (17 March 1999, event no. 20380677 from PIDC). The figure is in the same format as Figure 1. Contours of constant confidence level correspond to confidence regions on the hypocenter (top images) and epicenter (bottom images). The circles mark the event hypocenter reported in the Reviewed Event Bulletin.